Construction and Building Materials 158 (2018) 149–163

Contents lists available at ScienceDirect

Construction and Building Materials

journal homepage: www.elsevier.com/locate/conbuildmat

Experimental investigation of flexural behavior of glulam beams reinforced with different bonding surface materials

Murat Uzel [a], Abdullah Togay [b], Özgür Anil [c,*], Cevdet Söğütlü [d]

[a] Hacettepe Ankara Chm. of Industry 1st Organized Indst. Zone Voc. School, Ankara, Turkey
[b] Gazi University, Department of Industrial Design, Ankara, Turkey
[c] Gazi University, Civil Engineering Department, Ankara, Turkey
[d] Gazi University, Faculty of Technology, Department of Wood Products Industrial Engineering, Ankara, Turkey

HIGHLIGHTS

- Flexural behaviors of glue laminated timber beams.
- Number of laminations, types of adhesive materials and reinforcement nets used in the lamination surfaces.
- Use of reinforcement nets at the lamination surfaces increased the ultimate load capacities.
- Finite element simulations of some test specimens were performed.

ARTICLE INFO

Article history:
Received 1 July 2017
Received in revised form 29 September 2017
Accepted 5 October 2017
Available online 12 October 2017

Keywords:
Glulam beam
Bonding
Strengthening
Bending
Bond strengthening
ANSYS

ABSTRACT

In this study, flexuralbehaviors of glue laminated timber beams manufactured from Pinussylvestristree were investigated by comparing the results with those of massive timber beams. The main variables considered in the study were number of laminations, types of adhesive materials and reinforcement nets used in the lamination surfaces. In scope of the experimental study, glue laminated beams with 5 and 3 lamination layers were manufactured with 90 x 90 mm beam sections. In the lamination process epoxy and polyurethane glue were used. Morever, in order to improve the bond strength at the lamination surface, aluminium, fiberglass and steel wire nets were used at the lamination surfaces. Load–displacement responses, ultimate capacities, ductility ratios, initial stiffness, energy dissipation capacities and failure mechanisms of glue laminated beams were compared with those of massive beams. It was observed that the general bending responses of glue laminated beams were better than those of massive beams. In addition to that the use of reinforcement nets at the lamination surfaces increased the ultimate load capacities of the tested beams. The highest ultimate load capacities were oberved from the tests of glue laminated beams manufactured using five laminated layers and retrofitted with polyurethane glue using steel wire reinforcement nets, in the direction normal to the lamination surface. Finally, the finite element simulations of some test specimens were performed to observe the accuracy of finite element technology in the estimation of ultimate capacities of glue laminated timber beams.

1. Introduction

Timber is a material with high thermal and acoustic insulation properties with varying colors and fiber structures. It has been used for centuries due to its high strength/weight ratio as well as its aesthetic properties, easy processing, fiber structure, excellent thermal and sound insulation and better durability properties compared to other materials used as building materials [11]. It also has many positive environmental features including low buried energy, low carbon impact and sustainability [5]. Owing to these features, timber is a material used in the construction of beams, columns, roof trusses, poles, construction systems such as piles, slab elements, railway bases, and to give shape to concrete [11].

In North America, timber was used as the main structural material in most of the houses and commercial buildings before the 20th century. The abundance of timber resources is the foundation for most of the homes, commercial buildings, bridges and electricity poles. Today, houses and light commercial and industrial buildings are built using modern timber structural materials [14].

* Corresponding author.
E-mail address: oanil@gazi.edu.tr (Ö. Anil).

https://doi.org/10.1016/j.conbuildmat.2017.10.033
0950-0618/

Conversion factors

1 mm	0.039 in
1 mm^2	0.00152 in^2
1 kN	0.2248 kips
1 MPa	145 psi

Symbols

a	Distance between to support and loading, shear span length
h	Beam height
ρ_k	Charectheristic Density
ρ_{12}	Density
β_r	contraction coefficient
β_t	contraction coefficient
β_v	contraction coefficient
$E_{0,mean}$	Mean modulus of elasticity for perpendicular loading
$f_{m,k}$	Charectheristic bending strength
$f_{t,0,k}$	Charectheristic tension strength
$f_{c,0,k}$	Charectheristic compression strength
G_{mean}	Mean shear modulus for perpendicular loading

Wooden materials are still widely used today in settlement, commercial and industrial buildings, as well as in various constructions such as scaffoldings, bridges, retaining walls and power transmission towers. For example, in the United States, 90% of homes are timber [15].

In practice, the maximum possible span of the structural timber beams is limited to 5.0–7.0 m since the maximum size of the timber harvested from the logs is 300 mm depending on the tree species and the growing area. Before timber engineering products emerge, wooden trusses have been widely used to cross above the wide spans that are often required in the construction of roofs and bridges. Wooden trusses produced from timber are still the most common solutions for roofing in small houses. Wooden roof trusses are often used for spans up to 12.0 m, but can also be designed for openings up to 30.0–40.0 m [23].

Today, instead of using wood material directly, the use of wood based composite materials is preferred. Structural composite timber has been developed to reduce the consumption of forest resources and to meet the increasing demand for high quality timber. Structural composite timber is being used as a replacement for raw timber in the manufacture of engineering wood products such as prefabricated wooden I-beams and in other various applications to benefit from higher engineering design values than those offered by the raw timber [20]. Structural systems based on flat and sloping glue laminates have been developed for roofs with spans up to 100.0 m. Today, many other wood based products such as Laminated Veneered Lumber (LVL) and Parallel Strip Lumber (PSL) are used for large-scale timber constructions. Similarly, these products are suitable for larger spans, such as flat glued laminate timber elements [23]. Glue laminated timber started to be used in the late 1800 s. It was used extensively during and after World War II. Use of glue laminated beams (glulam beam) increase both in buildings and bridges. Structures cannot be erected using only saw timber proved the practical and successful aspects of glued laminated beams [21]. Wooden structures have also grown in size with the development of technology and the use of wooden building elements increased in different application fields such as bridges, sports facilities and industrial facilities besides the structures. The most important parameter affecting the load bearing capacity and general behavior of the timber laminated beams is the adherence of the laminated elements with each other. Several researches have been performed on this subject [19,22,4]. For larger spans, the design of laminated timber beams by reinforcing them with various composite materials has gain importance. The investigations have shown that researches on reinforcing timber laminated beams with composite materials such as CFRP are available in the literature [12,7,17,18]. In addition, there are studies in which steel elements are supported by wooden elements [24] or strengthened by prestressing [9,2,3,25].

In this study, it was aimed to use reinforcement elements produced from aluminum, fiberglass and steel materials in order to strengthen the bond between the two laminates of the beams to increase their performance under the effect of reversed cyclic loads such as seismic loads. From the literature review, it is observed that the externally bonded steel elements, CFRP elements and steel prestressing elements used for the strengthening of timber laminated beams. However, there are no studies in the literature on the use of retrofitting elements (fiber, aluminum, steel etc.) produced from various materials used to increase the bond between timber layers. For this reason, an experimental study was planned to investigate the effects of such bonding elements on the flexural behavior of glue laminated timber beams, which will increase the bond strength in the adhesion zone. The variables considered in the experimental study are: (i) the thickness, and (ii) number of laminates used in timber beams, (iii) the type of adhesive to be used on the bonding surface, (iv) the type of nets used to increase the bond strength on the bonding surface, (v) and the flexural load applied to the timber beams (i.e., perpendicular or parallel to the lamination surface). In order to examine the effects of the considered variables on the flexural behavior, timber beams were produced and tested under the effect of four point bending load. The ultimate load capacities, initial stiffnesses, displacement ductilities, energy dissipation capacities, failure mechanisms and general load displacement behaviors obtained from the experiments are analyzed and the effects of the strengthening method on the flexural behavior of the glulam beams are interpreted. In addition, nonlinear finite element analyzes of the test specimens were performed using the ANSYS finite element software and the numerical results were compared with the experimental results in terms of load-displacement behavior.

2. Experimental program

2.1. Test specimens and material

In the experimental study, flexural behavior of timber glue laminated beams is investigated. Variables considered in the study are: (i) the number, (ii) and thickness of laminates, (iii) the type of glue used to bond timber laminates, (iv) the netting type used to strengthen the lamination zones to improve the bending behavior of timber laminated beams, (v) and the flexural load applied to timber beams (i.e., parallel and perpendicular to the lamination surfaces). In order to determine the effects of the net types on the flexural behavior, massive beams that were not laminated are also produced and the obtained results are compared with those of retrofitted glue laminated beams. In the experimental program, a total of $33 \times 3 = 99$ timber beams are produced from 33 main timber beams (i.e., 3 beams for each type) and four point monotonic bending loading is applied to the test specimens. The properties of the test elements are given in Table 1.

The timber beams are 90×90 mm in size and 1710 mm in length. Tests of the specimens and determination of their properties were performed in accordance with EN 13183-1. The geometric dimensions of the test specimens are given in Fig. 1 in relation

to the beam height (i.e., h = 90 mm). Laminated timber beams are produced from 3 to 5 layers of 30 mm and 18 mm thickness. Two different types of adhesives: (i) epoxy and (ii) polyurethane are used in the lamination procedure. Three different types of materials (i.e., fiber, aluminum and steel) are used to strengthen the lamination surfaces. Loading in the tests of the specimens were applied in directions normal and parallel to the bonding surfaces.

In the scope of experimental study, Pinussylvestris timber, which is widely used in timber construction sector, was used. Attention has been paid to prevent to presence of wood defects such as knots, cracks and fiber imperfections in the timbers used in the tests. Table 2 presents the physical and mechanical properties of the Pinus sylvestris tree used in the study. Two different types of glue were used to prepare the test specimens (i.e., polyurethane and epoxy). Polyurethane adhesive is highly elastic and has high resistance to water, chemical substances, oils and microorganisms. Polyurethane adhesive used in the production of timber structural elements is a one-component D4 type reactive adhesive that is cured with airborne moisture curing. The high temperature resistances of Polyurethane adhesives are stated for their ability in resisting external heat effects such as fires. The material to be glued with polyurethane adhesive should be dry, free from dust and oil. Material humidity should be the range of 8–12%. The specifications of the polyurethane glue used in the study are given in Table 3.

Epoxy compounds used in the production of epoxy glue are obtained in the petrochemical industry. The drying, curing and bonding properties of the two-component epoxy adhesive depend on the chemical structure of the components. During the reaction, no materials evaporate or leave the glue. The surface must be sanded before the application of the epoxy. The parts A and B of epoxy are mixed together at a ratio of 1/1, and the mixture is mixed until it becomes homogeneous. After 5 min, the adhesive is applied to both surfaces to be bonded with a spatula or brush. The two surfaces are pressed for 24 h. Care must be taken that the room temperature is at least 15 °C. The technical properties of the epoxy glue used in the study are given in Table 4.

Three types of nets were used in the study; (i) to improve the strength on the bond surfaces of the laminates forming the timber beams and, (ii) to improve the flexural behavior by strengthening the test elements. These nets are made from fiber, aluminum and steel materials. Aluminum wire mesh net is produced from 0.28 mm thickness wire which is durable, long life, non-deformed, bright colored and has 18 × 16 mm openings. In addition, these nets have stainless features. The fiberglass wire mesh used between laminates is 125 gr/m^2 and contains 35% fiberglass and 65% plastic. The fiberglass wire mesh is made of high quality and twisted yarn in 0.28 mm thickness. Fiberglass wire mesh opening spacing is 16 × 18 mm. The steel wire used for strengthening the test specimens is a standard steel wire net used in the plastering applications. Three types of wire mesh used in the study are presented in Fig. 2.

In the production of massive single-piece beam test specimens, the beams were firstly cut to 105 × 105 × 1800 mm and then kept until 12% moisture at 20 ± 2 °C temperature and 65 ± 5% relative humidity conditions without exposition to direct sunlight. The timbers which reached to the air-dry humidity were cut in net size of 90 × 90 × 1710 mm.

Laminates of 25 and 35 mm thicknesses of various lengths and widths obtained from Pinus sylvestris, which are free from defects such as cracks, knots and resin cuts, are stacked in such a way that they are not exposed to direct sunlight and have a temperature of 20 ± 2 °C and a relative humidity of 65 ± 5%. They were kept until reaching 12% moisture content. On the laminates, reaching equilibrium humidity, a face and oriels were firstly opened on the planer and then brought to a thickness of 18 and 30 mm in the thickness

Table 1
Properties of test specimens.

Spec No.	Definition	Loading Direction	Glulam Layer Number	Bonding Materials	Strengthening Material
1	PER_3ER	Perpendicular to Glulam Layer	3	Epoxy	Reference
2	PER_3EA				Aliminum net
3	PER_3EF				Fiberglass net
4	PER_3ES				Steel net
5	PER_3PR			Poly-Uratane	Reference
6	PER_3PA				Aliminum net
7	PER_3PF				Fiberglass net
8	PER_3PS				Steel net
9	PER_5ER		5	Epoxy	Reference
10	PER_5EA				Aliminum net
11	PER_5EF				Fiberglass net
12	PER_5ES				Steel net
13	PER_5PR			Poly-Uratane	Reference
14	PER_5PA				Aliminum net
15	PER_5PF				Fiberglass net
16	PER_5PS				Steel net
17	PAR_3ER	Parallel to Glulam Layer	3	Epoxy	Reference
18	PAR_3EA				Aliminum net
19	PAR_3EF				Fiberglass net
20	PAR_3ES				Steel net
21	PAR_3PR			Poly-Uratane	Reference
22	PAR_3PA				Aliminum net
23	PAR_3PF				Fiberglass net
24	PAR_3PS				Steel net
25	PAR_5ER		5	Epoxy	Reference
26	PAR_5EA				Aliminum net
27	PAR_5EF				Fiberglass net
28	PAR_5ES				Steel net
29	PAR_5PR			Poly-Uratane	Reference
30	PAR_5PA				Aliminum net
31	PAR_5PF				Fiberglass net
32	PAR_5PS				Steel net
33	Massive	Reference (without glulam one piece)			

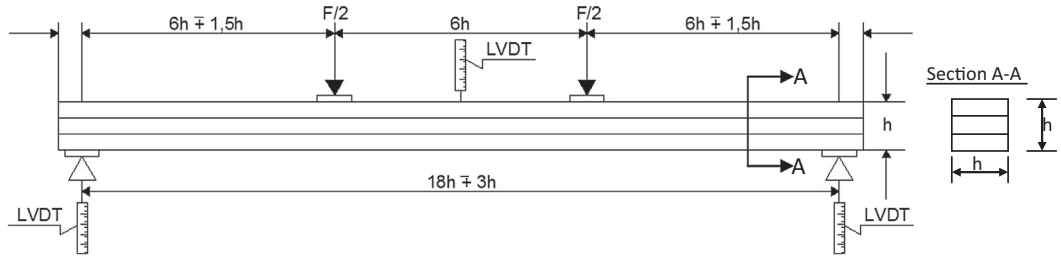

a) Loading direction is perpedicular to Glulam

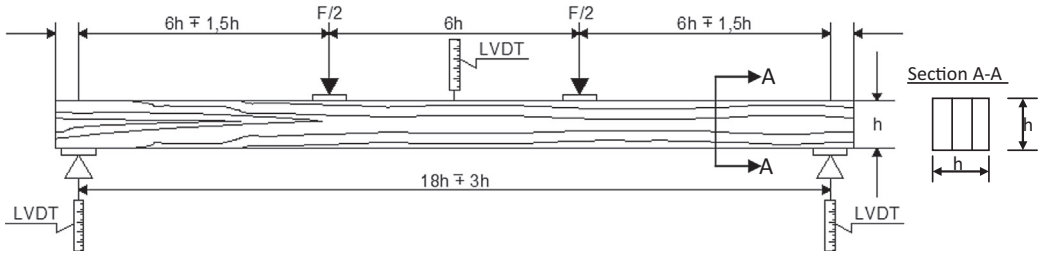

b) Loading direction is parallel to Glulam

Fig. 1. Dimensions of test specimens.

Table 2
Mechanical properties of pinussylvestris.

Remarks	Symbol	Value	Unit
Density	ρ_k	490	kg/m^3
	ρ_{12}	520	kg/m^3
Contraction coefficient	β_r	4.0	%
	β_t	7.7	%
	β_v	12.1	%
Elastic Modulus	$E_{0,mean}$	11700	MPa
Shear Modulus	G_{mean}	731.25	MPa
Bending strength	$f_{m,k}$	98	MPa
Tension strength	$f_{t,0,k}$	102	MPa
Compression strength	$f_{c,0,k}$	54	MPa

Table 3
Technical properties of polyurethane glue.

Properties	Remarks
Base	Polyurethane
Specific weight	0.0011 + 0.0002 kg/m^3
Brookfieldsp 3/20 rpm	1600 + 0.02 m Pa's
Density	liquid
Working temperature	Optimal working temperature 20 °C
	Minimum working temperature 5 °C
Compressive Strength	60 MPa
Tensile strength	26.2 MPa
Elastic Modulus	830 MPa
Elongation at break	13%

Table 4
Technical properties of epoxy glue.

Properties	Values
Solid material in volume (%)	100
Density	1.1
Dry film thickness (mm)	0.2
Working temperature (°C)	+15 to +35
Compressive Strength	190 MPa
Elastic Modulus	10500 MPa
Tensile Strength	85 MPa
Elongation at break	0.8%

machine. Five timber layers with parallel fiber directions of 18 mm in thickness and three timber layers in 30 mm thickness are fixed to each other with epoxy or polyurethane glue. It should be noted that 3 identical test samples are produced for each test specimen. In the tests aluminum wire mesh, fiber wire mesh and steel wire mesh were placed between the adhesive surfaces of the laminates. Examples of photographs taken during the production phase of the test elements are given in Fig. 3.

2.2. Test setup and instrumentation

Timber beam test specimens produced in scope of the experimental study were tested by applying four point flexural load to examine the behavior under bending load. The loading on the test elements was monotonically increased from zero to collapse. Four point loading were applied by choosing the distance between load and the support points (a) as 6 times of the beam height (h) to have a bending dominated behavior. The test elements were loaded with a 600 kN capacity hydraulic jack and the measurements were taken by using a 400 kN capacity load cell. A total of 3 displacement measurements were taken from midpoint and two support points. The displacement of the midpoint of the test elements was corrected using the displacement measurements at supports. The tests were performed by following the mid-point displacement loading plots and the results were interpreted by calculating the ultimate capacity, initial stiffness, displacement ductility ratio and energy dissipation capacity values using the load-midpoint displacement graphs. The load and displacement values measured from the test elements were collected by a data collection system and transferred to the computer to evaluate the test results. The experiment and measurement setup used in the experiments are shown in Fig. 4.

3. Experimental results and evaluations

3.1. Observed behavior and failure modes

In the experimental study, 33 different types of beam specimens were produced and a total of 99 (i.e., 3 identical specimens

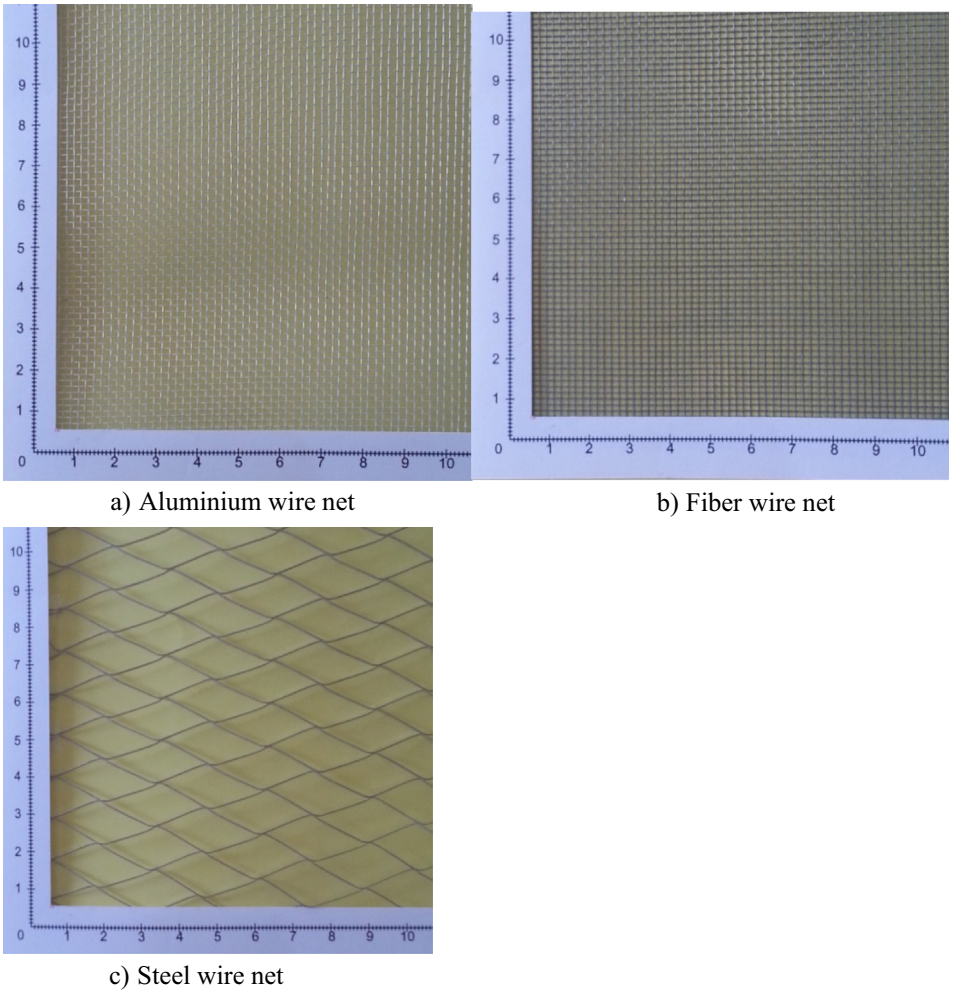

Fig. 2. Wire nets used in the retrofitting procedure.

are manufactured for each beam) beam specimens were tested by applying four point bending load test. Variables considered in the experimental study are (i) the number and (ii) thickness of the laminates used in the production of specimens, (iii) the type of adhesive used in the bonding process, (iv) the type of net used on the bonding surface and (v) the application of the loading in parallel or normal to the bonding surface. All results obtained from the experimental study are given in Table 5. In Table 5, the values given for each type of beam specimens were calculated by taking the average of the test results of the three identical test specimens. The standard deviations and variance values of the three identical test specimens produced for each beam are very small and the experimental results obtained from three identical samples are very close to each other. As a result of the tests, the load-displacement plots of the test specimens are obtained and using these plots, the ultimate load values, displacement ductility ratios, energy dissipation capacities and initial stiffness values are calculated. In Fig. 5, selected examples of load-displacement graphs are shown. Selected examples of photographs showing the damage distribution on the beams after the tests are presented in Fig. 6.

The maximum strength of the beams tested in the experimental study is defined using the maximum load value reached by the load-displacement graphs. The initial stiffness values are obtained by proportioning the load value of the point of first significant change in the slope to the displacement value of same point. The displacement ductility ratios of the test specimens are calculated using load-displacement relationships. The displacement ductility ratios are calculated by the ratio of displacement of the point of failure to that of the point at which the sudden change in the point of collapse. The point of collapse is defined by the point at which the maximum load value of the test specimens decrease by 15%. The energy dissipation capacities of the test specimens are calculated using the area under the load-displacement relationships. The energy dissipation capacities are obtained by calculating the area under the load-displacement graph section up to the point of failure of the test specimens, and the point of failure is the point determined for calculating the displacement ductility ratios. Calculation of load resisting capacities, initial stiffnesses, displacement ductility ratios and energy dissipation capacities are illustrated in Fig. 7.

In the experimental study, the effect of the strengthening technique on the important structural parameters was investigated by comparing the results of massive test specimen with those of the laminated test specimens. The ultimate load capacities, initial stiffnesses and energy dissipation capacities of non-reinforced laminated test specimens were obtained 9%, 6% and 29% higher than those of the massive specimen, respectively. However, the displacement ductility ratio of massive specimen is 8% larger than that of laminated non-retrofitted beams. The four most important parameters (i.e., the ultimate load capacity, the displacement ductility ratio, the initial stiffness and the energy dissipation capacity) of the test specimens retrofitted using nets were significantly

Fig. 3. Chosen photo samples from the manufacturing process of test specimens.

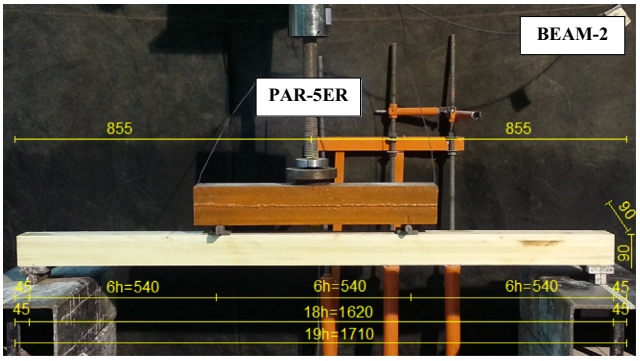

Fig. 4. Test and measurement devices setup.

higher than those of the massive test member. The ultimate load capacity, displacement ductility ratio, initial stiffness and energy dissipation capacities of the beams retrofitted using aluminum nets were obtained 36%, 13%, 23% and 36%higher than those of the massive beam, respectively. These ratios were 49%, 20%, 28% and 44% for fiber net retrofitted glue laminated beams and 55%, 28%, 33% and 62% for steel net retrofitted glue laminated beams. In the study, the maximum increase in the ultimate load capacities, displacement ductility ratios, and initial stiffness and energy dissipation capacities of the beams was observed in the test specimens retrofitted using steel wire nets.

The increase in the number of the laminate due to the decrease in the thicknesses of layers led to an increase in the displacement ductility ratio, initial stiffness and the energy dissipation capacity. Increase of laminate number from 3 to 5 lead to a 6% increase in the ultimate load capacity, 10% increase in the displacement ductility ratio, 3% increase in the initial stiffness value and 19% increase in the energy dissipation capacities. For the perpendicular loading case, as the number of layers increases, the collapse occurs due to: (i) the exceedance of the tensile strength of the layer on the tension surface and (ii) the separation of laminates from the adhesive surface near the tension surface.

Table 5
Experimental results.

Spec. No	Definition	Ultimate Capacity (kN)	Displacement Ductility Ratio	Initial Stiffness (kN/mm)	Energy Dissipation Capacity (kN-mm)	Failure Mode
1	PER_3ER	29.73	1.44	1.09	1280.93	Tension face rupture
2	PER_3EA	34.57	1.83	1.30	1385.81	Tension face rupture
3	PER_3EF	35.79	1.85	1.35	1415.12	Tension face rupture
4	PER_3ES	38.22	1.89	1.43	1460.14	Tension face rupture
5	PER_3PR	29.70	1.43	1.07	1220.27	Tension face rupture
6	PER_3PA	37.27	1.67	1.27	1319.83	Tension face rupture
7	PER_3PF	44.03	1.78	1.31	1353.86	Tension face rupture
8	PER_3PS	45.85	1.83	1.36	1427.8	Tension face rupture
9	PER_5ER	29.83	1.52	1.17	1499.6	Tension face rupture and debonding
10	PER_5EA	39.17	2.20	1.32	1554.99	Tension face rupture and debonding
11	PER_5EF	42.91	2.42	1.38	1760.49	Tension face rupture and debonding
12	PER_5ES	45.12	2.52	1.44	2313.47	Tension face rupture and debonding
13	PER_5PR	29.81	1.47	1.14	1460.04	Tension face rupture and debonding
14	PER_5PA	40.63	1.88	1.31	1524.69	Tension face rupture and debonding
15	PER_5PF	44.41	1.91	1.36	1617.43	Tension face rupture and debonding
16	PER_5PS	46.02	2.21	1.39	2071.59	Tension face rupture and debonding
17	PAR_3ER	29.50	1.43	1.08	1145.51	Tension face rupture
18	PAR_3EA	33.97	1.69	1.28	1209.06	Tension face rupture
19	PAR_3EF	34.49	1.81	1.31	1267.5	Tension face rupture
20	PAR_3ES	35.78	1.86	1.41	1377.34	Tension face rupture
21	PAR_3PR	29.53	1.42	1.06	1130.45	Tension face rupture
22	PAR_3PA	36.21	1.65	1.26	1198.05	Tension face rupture
23	PAR_3PF	40.75	1.77	1.30	1256.34	Tension face rupture
24	PAR_3PS	41.55	1.82	1.35	1346.23	Tension face rupture
25	PAR_5ER	29.61	1.49	1.16	1471.34	Tension face rupture
26	PAR_5EA	34.44	1.75	1.31	1512.56	Tension face rupture
27	PAR_5EF	38.73	1.86	1.37	1598.12	Tension face rupture
28	PAR_5ES	39.10	2.12	1.43	1644.4	Tension face rupture
29	PAR_5PR	29.63	1.46	1.13	1350.25	Tension face rupture
30	PAR_5PA	39.36	1.72	1.29	1476.34	Tension face rupture
31	PAR_5PF	42.21	1.85	1.35	1520.34	Tension face rupture
32	PAR_5PS	45.14	2.09	1.38	1640.34	Tension face rupture
33	Massive	27.18	1.59	1.05	1026.91	Tension face rupture

In the 5-layered test specimens, the failure occurred due to a combination of the separation and fracture of the layers. In the 3-layered test specimens, the collapse occurred only by the failure of the layer near the tension surface. When the loading is applied parallel to the laminates, no separation is observed on the bonding surfaces and the failure occurred due to breaking of the fibers near the tension surface for both 5-layered and 3-layered test specimens. The separation on the bond surface was observed only in the proximity of the broken fiber.

Another variable that is examined in the experimental study is the loading direction. The application of the bending load in perpendicular direction to the layers caused the maximum values of ultimate load capacity, displacement ductility ratio, initial stiffness and energy dissipation capacity to increase. Perpendicular loading lead to an increase: (i) in the maximum load by 5%, (ii) in the displacement ductility by 7%, (iii) in the initial stiffness by 1% and (iv) in the energy consumption capacity by 11%.

Another variable that is examined is the type of adhesive used to bond the layers. The bonding of the layers with the polyurethane adhesive results in an increase in the ultimate load value, a decrease in the displacement ductility ratio, a decrease initial stiffness and energy dissipation capacity values when compared with those of the elements bonded by using the epoxy adhesive. The ultimate load capacities of the test specimens bonded with the polyurethane adhesive was 8% larger than those of the specimens bonded by using the epoxy adhesive. The displacement ductility ratio, the initial stiffness and the energy dissipation capacity values were 6%, 2% and 4%, lower than those of the specimens bonded by using the epoxy adhesive, respectively.

The last variable examined in the experimental study is the net type used on the adhesion surfaces between the layers. In the experimental study, the most effective reinforcement net type showed variability as a function of considered structural parameters. The values of ultimate load capacity, displacement ductility ratio, initial stiffness and energy dissipation capacity increased with the use of a net at the bonding surface. Among the three types of materials used as net material, the least increase was obtained with aluminum wire netting and the most increase was obtained with steel wire netting. Test specimens retrofitted using fiberglass mesh material showed a performance between these two net types. The use of a net on the surface provided a34% increase on ultimate load capacity, 31% increase on displacement ductility, 21% increase on initial stiffness and 14% increase on energy dissipation capacity, in average.

3.2. Strength and stiffness

The greatest effect on the maximum strength values occurred due to the use of nets in the lamination layers. In the case of the 3-layer test specimens with epoxy adhesive and loaded perpendicular to the lamination surfaces, the ultimate load increased by 16%, 20% and 29% for aluminum, fiber and steel wire nets, respectively, with respect to the non-retrofitted specimen. In the case of the 3-layer test specimens with polyurethane adhesive and loaded perpendicular to the lamination surfaces, the ultimate load increased by 25%, 48% and 54% for aluminum, fiber and steel wire nets, respectively, with respect to the non-retrofitted specimen. In the case of the 5 layer test specimens with epoxy adhesive and loaded perpendicular to the lamination surfaces, the ultimate load increased by 31%, 44%, 51% for aluminum, fiber and steel wire nets, respectively, with respect to the non-retrofitted specimen. For the 5 layer test specimens with polyurethane adhesive and loaded perpendicular to the lamination surfaces, the maximum load increased by 36%, 49%, and 54% for aluminum, fiber and steel wire

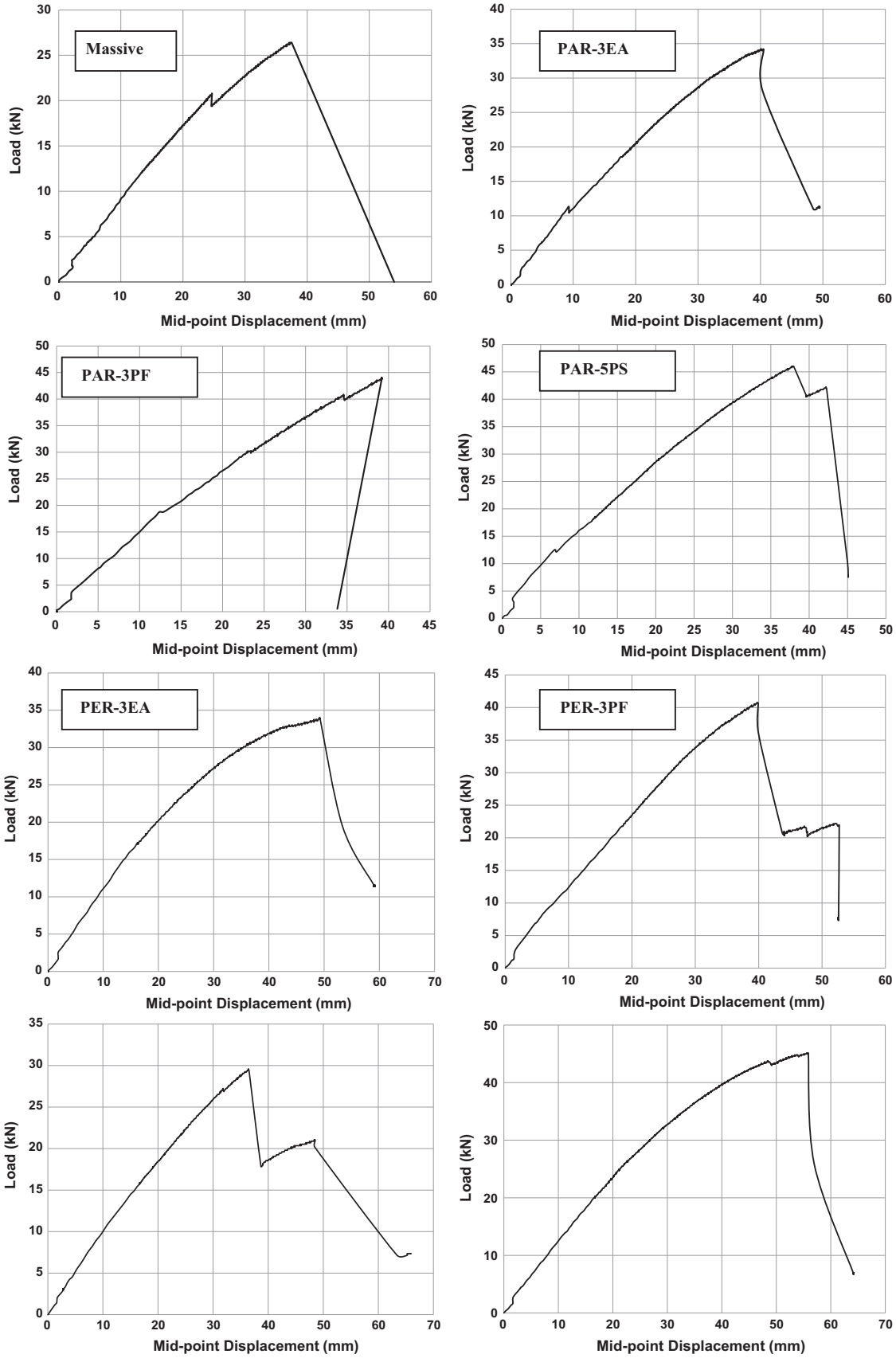

Fig. 5. Samples from the load-displacement relationships of the test specimens.

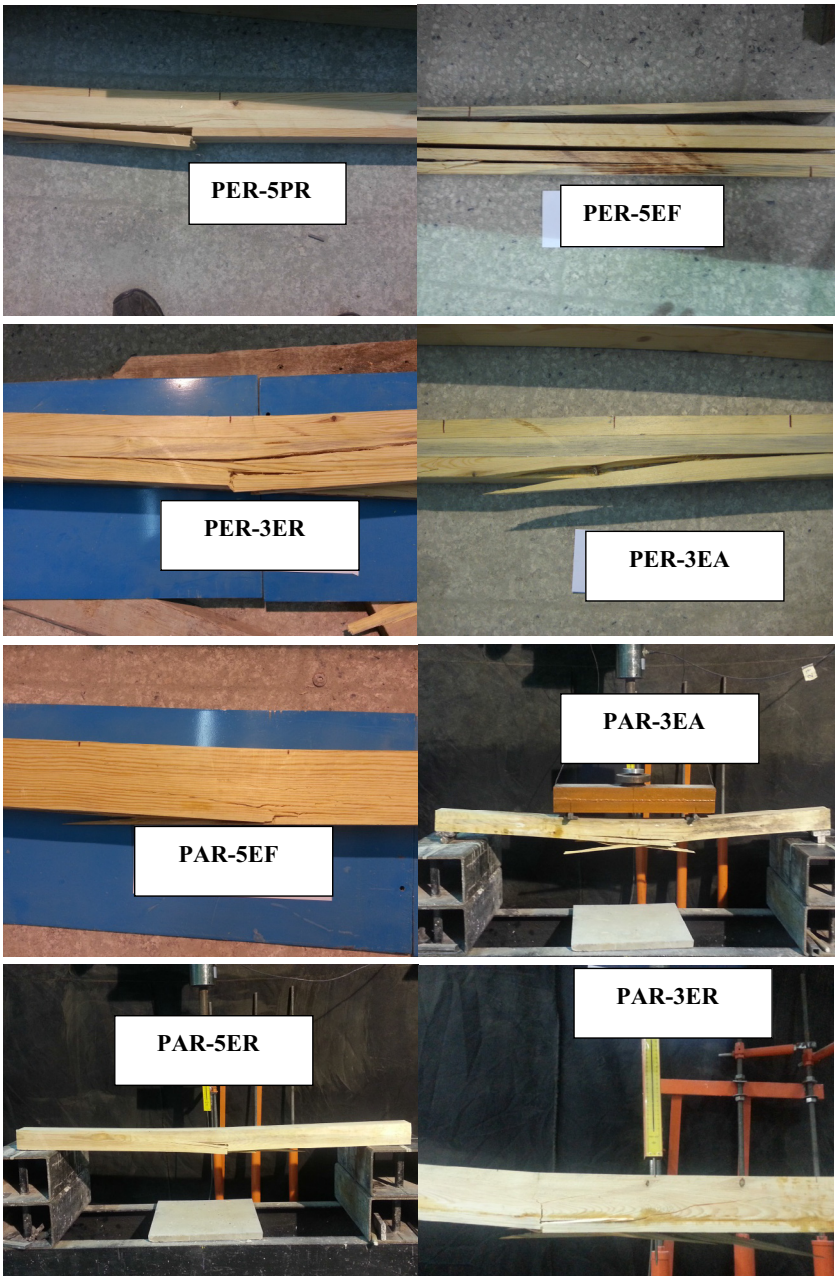

Fig. 6. Samples from the failed conditions of the test specimens.

nets, respectively, with respect to the non-retrofitted specimen. In the case of the 3-layer test specimens with epoxy adhesive and loaded parallel to the lamination surfaces, the maximum load increased by 15%, 17% and 21%, for aluminum, fiber and steel wire nets, respectively, with respect to the non-retrofitted specimen. In the case of the 3-layer test specimens with polyurethane adhesive and loaded parallel to the lamination surfaces, the ultimate load increased by 23%, 38% and 41%, for aluminum, fiber and steel wire nets, respectively, with respect to the non-retrofitted specimen. In the case of the 5-layer test specimens with epoxy adhesive and loaded parallel to the lamination surfaces, the ultimate load increased by 16%, 31% and 32%, for aluminum, fiber and steel wire nets, respectively, with respect to the non-retrofitted specimen. For 5-layer test specimens with polyurethane adhesive and loaded parallel to the lamination surfaces, the ultimate load increased by 33%, 42% and 52%, for aluminum, fiber and steel wire nets, respectively, with respect to the non-retrofitted specimen.

Use of polyurethane adhesive resulted in higher ultimate load values in comparison to the test specimens manufactured using epoxy adhesive. Strength value of specimen manufactured with 3 layers and polyurethane adhesive, retrofitted with aluminum mesh and loaded perpendicular to the layers is 7% higher than its counterpart manufactured using epoxy adhesive. This ratio is 19% for the fiber-reinforced test specimen and 17% for the steel-wire retrofitted test specimen. Ultimate load value of specimen manufactured with 5 layers and polyurethane adhesive, retrofitted with aluminum mesh and loaded perpendicular to the layers is 4% higher than its counterpart manufactured using epoxy adhesive. This ratio is 3% for the fiber-reinforced test specimen and 2% for the steel-wire retrofitted test specimen. Ultimate load value of

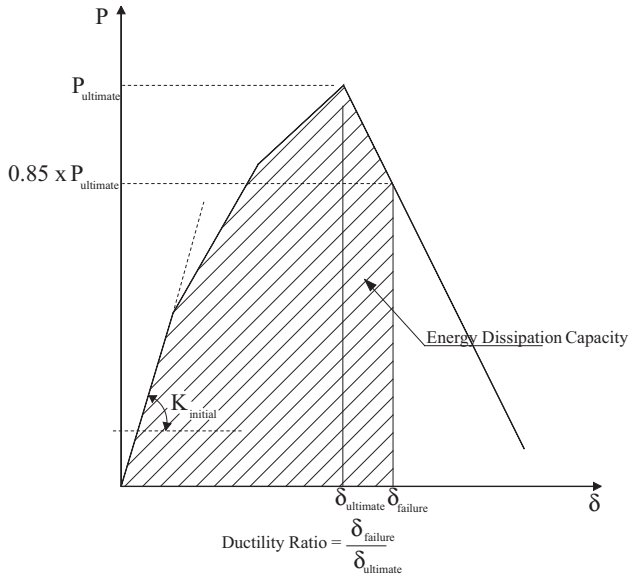

Fig. 7. Calculation approach of Ultimate Load Capacity, Intial Stiffness, Displacement Ductility Ratios and Energy Dissipation Capacity.

specimen manufactured with 3 layers and polyurethane adhesive, retrofitted with aluminum mesh and loaded parallel to the layers is 6% higher than its counterpart manufactured using epoxy adhesive. This ratio is 15% for the fiber-reinforced test specimen and 14% for the steel-wire test specimen. Ultimate load value of specimen manufactured with 5 layers and polyurethane adhesive, retrofitted with aluminum mesh and loaded parallel to the layers is 13% higher than its counterpart manufactured using epoxy adhesive. This ratio is 8% for the fiber-reinforced test specimen and 13% for the steel-wire retrofitted test specimen. The load bearing capacities of test specimens with Polyurethane adhesives are 8% larger than those of specimens with epoxy adhesives. The fluidity of Polyurethane adhesive is more than the two compound epoxy adhesive. In relation to that the absorption of Polyurethane adhesive in the layers are more pronounced than the epoxy adhesive. The more solid form of epoxy adhesive decreased the connection between the timber layers and nets and also prevented its uniform distribution. It is believed that these factors contributed to the difference in the load bearing levels

The change in the orientation of the load and the change in the number of layers were less effective on the ultimate load capacity of the test specimens than the reinforcement material and adhesive type. The perpendicular loading increased the strength values with respect to the parallel loading at a low amount. Increasing the number of layers from 3 to 5 also increases the load ultimate load, but this increase is not notable with respect to the effect of reinforcing material type and the adhesive type.

The most effective factor on the variation of initial stiffness values is the type of the net used in the retrofitting procedure. The effects of number of layers, the adhesive type and the loading condition on the initial stiffness were less pronounced. The initial stiffness values of the test specimens that were manufactured using polyurethane were smaller than those of manufactured using epoxy. The initial stiffness values of the test specimens loaded perpendicular to the layers were larger than those of the test specimens loaded in parallel. The increase of the number of layers increased the initial stiffness values. The five-layered test specimens have larger initial stiffness than the three-layered test specimens.

The initial stiffness values of the test specimens reinforced with aluminum, fiber and steel nets using 3 layer and epoxy adhesive, loaded perpendicular to the layers were calculated as 19%, 24% and 31%, respectively, larger than that of the non-reinforced test specimens. The initial stiffness values of the test specimens reinforced with aluminum, fiber and steel nets using 3 layer and polyurethane adhesive, loaded perpendicular to the layers were calculated as 19%, 22% and 27% larger than that of the non-reinforced test specimens, respectively. The initial stiffness values of the beam test specimens reinforced with aluminum, fiber and steel nets using 5 layer and epoxy adhesive, loaded perpendicular to the layers were calculated as 13%, 18% and 23%, respectively, larger than that of the non-reinforced test specimens. The initial stiffness values of the test specimens reinforced with aluminum, fiber and steel nets using 3 layer and polyurethane adhesive, loaded perpendicular to the layers were calculated as 15%, 19% and 22% larger than that of the non-reinforced test specimens, respectively.

The initial stiffness values of the beam test specimens reinforced with aluminum, fiber and steel nets using 3 layer and epoxy adhesive, loaded parallel to the layers were calculated as 19%, 21% and 31%, respectively, larger than that of the non-reinforced test specimens. The initial stiffness values of the test specimens reinforced with aluminum, fiber and steel nets using 3 layer and polyurethane adhesive, loaded parallel to the layers were calculated as 19%, 23% and 27% larger than that of the non-reinforced test specimens, respectively. The initial stiffness values of the beam test specimens reinforced with aluminum, fiber and steel mesh using 5 layer and epoxy adhesive, loaded parallel to the layers were calculated as 13%, 18% and 23%, respectively, larger than that of the non-reinforced test specimens. The initial stiffness values of the test specimens reinforced with aluminum, fiber and steel nets using 3 layer and polyurethane adhesive, loaded parallel to the layers were calculated as 14%, 19% and 22% larger than that of the non-reinforced test specimens, respectively.

3.3. Displacement ductility ratio

In the experimental study, the change in the number of layers and type of nets used at the bonding surface were more effective on the displacement ductility ratio, while the adhesive type and loading direction variables were less effective. The uses of nets as the reinforcing material and the increase in the number of layers have increased the displacement ductility ratio significantly. The displacement ductility ratios of the test specimens retrofitted using epoxy adhesive were calculated to be 6% larger than the test members retrofitted using polyurethane adhesive. In the test specimens loaded perpendicular to the layers, the displacement ductility ratios were obtained 7% more than the test elements loaded parallel to the layers, in average.

The most effective variable on the displacement ductility ratio is the type of reinforcement material. The change of the reinforcement material has caused a significant change in the displacement ductility ratios. The ductility ratios of the test specimens manufactured with 3 layers and strengthened with aluminum, fiber and steel nets using epoxy adhesive and loaded perpendicular to the layers were calculated as 27%, 28% and 31% larger than those of the non-retrofitted specimens, respectively. The ductility ratios of the test specimens manufactured with 3 layers and strengthened with aluminum, fiber and steel nets using polyurethane adhesive and loaded perpendicular to the layers were calculated as 17%, 24% and 28% larger than those of the non-retrofitted specimens, respectively. The ductility ratios of the test specimens manufactured with 5 layers and strengthened with aluminum, fiber and steel nets using epoxy adhesive and loaded perpendicular to the layers were calculated as 45%, 59% and 66% larger than those of the non-retrofitted specimens, respectively. The ductility ratios of the test specimens manufactured with 5 layers and strengthened with aluminum, fiber and steel nets using polyurethane adhesive

and loaded perpendicular to the layers were calculated as 28%, 30% and 50% larger than those of the non-retrofitted specimens, respectively.

The ductility ratios of the test specimens manufactured with 3 layers and strengthened with aluminum, fiber and steel nets using epoxy adhesive and loaded parallel to the layers were calculated as 18%, 27% and 30% larger than those of the non-retrofitted specimens, respectively. The ductility ratios of the test specimens manufactured with 3 layers and strengthened with aluminum, fiber and steel nets using polyurethane adhesive and loaded parallel to the layers were calculated as 16%, 25% and 28% larger than those of the non-retrofitted specimens, respectively. The ductility ratios of the test specimens manufactured with 5 layers and strengthened with aluminum, fiber and steel nets using epoxy adhesive and loaded parallel to the layers were calculated as 17%, 25% and 42% larger than those of the non-retrofitted specimens, respectively. The ductility ratios of the test specimens manufactured with 5 layers and strengthened with aluminum, fiber and steel nets using polyurethane adhesive and loaded parallel to the layers were calculated as 18%, 27% and 43% larger than those of the non-retrofitted specimens, respectively. The increase in the number of layers also caused a slight increase in displacement ductility ratios. The 5-layered test specimens exhibited 10% greater ductility ratio than the 3-layered test specimens, in average.

3.4. Energy dissipation capacity

The change in the number of layers and nets used at the bonding surface for strengthening led to a more pronounced variation in the energy dissipation capacities, while the adhesive type and loading direction variables were effective at a lower rate. The uses of nets as the reinforcing material and the increase in the number of layers have increased the energy dissipation capacities. The energy dissipation capacities of the test specimens retrofitted using epoxy adhesive were calculated to be 4% larger than those of the specimens retrofitted using polyurethane adhesive. The energy dissipation capacities of the test specimens loaded perpendicular to the layers are calculated by 11% more than the test specimens loaded parallel to the layers. The increase in the number of layers is the most effective variable on the values of energy dissipation capacities. The 5-layered test specimens exhibited an average energy dissipation capacity of 19% greater than the 3-layered test specimens.

The variation of the strengthening material types led to a variation in the energy dissipation capacity values. The energy dissipation capacity values of the 3 layered test specimens strengthened by aluminum, fiber and steel net using epoxy adhesive and loaded perpendicular to the layers were calculated 8%, 10% and 14% higher than the non-reinforced test specimens, respectively. The energy dissipation capacity values of the 3 layered test specimens strengthened by aluminum, fiber and steel net using polyurethane adhesive and loaded perpendicular to the layers were calculated 8%, 11% and 17% higher than the non-reinforced test specimens, respectively. The energy dissipation capacity values of the 5 layered test specimens strengthened by aluminum, fiber and steel net using epoxy adhesive and loaded perpendicular to the layers were calculated 4%, 17% and 54% higher than the non-reinforced test specimens, respectively. The energy dissipation capacity values of the 5 layered test specimens strengthened by aluminum, fiber and steel net using polyurethane adhesive and loaded perpendicular to the layers were calculated 4%, 11% and 42% higher than the non-reinforced test specimens, respectively.

The energy dissipation capacity values of the 3 layered test specimens strengthened by aluminum, fiber and steel net using epoxy adhesive and loaded parallel to the layers were calculated 6%, 11% and 20% higher than the non-reinforced test specimens, respectively. The energy dissipation capacity values of the 3 layered test specimens strengthened by aluminum, fiber and steel net using polyurethane adhesive and loaded parallel to the layers were calculated 6%, 11% and 19% higher than the non-reinforced test specimens, respectively. The energy dissipation capacity values of the 5 layered test specimens strengthened by aluminum, fiber and steel net using epoxy adhesive and loaded parallel to the layers were calculated 3%, 9% and 12% higher than the non-reinforced test specimens, respectively. The energy dissipation capacity values of the 5 layered test specimens strengthened by aluminum, fiber and steel net using polyurethane adhesive and loaded parallel to the layers were calculated9%, 13% and 21% higher than the non-reinforced test specimens, respectively.

4. Finite element analyses

In scope of the study also finite element simulations of specimens loaded perpendicular to the layers are performed. For this purpose half models of test specimens are constructed by using the symmetry conditions (Fig. 8). The analyses of the other test specimens are not performed due to the absence of a valid and trusted failure criteria required to terminate the analyses.

In the simulation procedure, 3375 finite elements are used for the simulation of the half models. A rectangular finite element mesh is used in the modeling procedure, with the dimensions of $19 \times 6 \times 19$ mm ($45 \times 15 \times 5 = 3375$ number of elements). From the preliminary mesh sensitivity analyses, it is observed that using elements with smaller dimensions did not notably affect the analyses results due to the fact that dimensions of the selected elements are already small enough.

In the finite element simulations, elastic steel loading and support plates are used at the support and loadingpoints. In the finite element modeling procedure the elastic steel plates and timber are modeled by using solid elements from the ANSYS library i.e., steel plates are modeled using SOLID185 and timber elements are modeled using SOLID45). SOLID45 used for the modeling of timber is used for the 3-D modeling of solid elements. The solid element has eight nodes with three degrees of freedom for each node [1]. SOLID45 has plasticity, stress stiffening, large deflection, and large strain and some other abilities node [1]. Similarly, SOLID185 is solid element similar to SOLID45 with some differences such as hyperelasticity [1]. As stated before, steel plates are modeled as

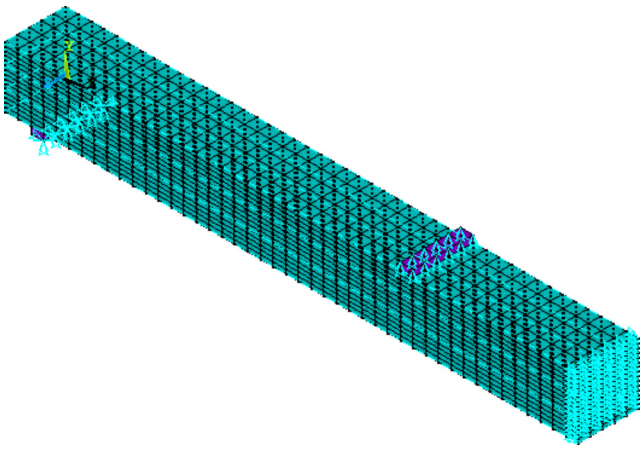

Fig. 8. Half model of the test specimens.

Table 6
Elastic material properties of steel plates.

Property	Value
Modulus of Elasticity	200 GPa
Poisson's Ratio	0.3

elastic. Elastic properties of the steel loading plates are given in Table 6.

However the accurate simulation of complex anisotropic behavior of timber is not a practical issue. In order to simulate the timber behavior, elastic and inelastic properties of the timber are defined in the software in orthogonal and anisotropic formats [16]. The material properties used in the simulation procedure are given in Fig. 9a and b, respectively for elastic orthotropic and anisotropic behaviors. It should be noted that the full material properties given in Fig. 9a and b are adopted from Pencik [16].

For the simulation of timber under the multiaxial stress conditions anisotropic hardening plasticity material model [13] is used together with material properties given in Fig. 9. In the models the failure of the simulated specimens is defined with the maximum stress failure criterion.

In the finite element simulations the analyses are stopped when the tensile stresses at the lowest lamination layer reaches to the 80% tensile strength capacity of the timber [10]. Since failure of timber elements below the outermost lamination generally do not lead to the complete failure of glue laminated beams [8].

The nets used in the retrofitting procedure are not directly modeled in the simulations, their tangential bond - slip relationships are used to simulate the delamination process in the lamination surfaces. For this purpose the shear stress-slip relationships of the tested specimens are used in the well known cohesive zone material (CZM) model. In the simulations only tangential separation of laminated layers are considered due to the fact that the behavior of test specimens are dominated by flexural mode and the relative vertical displacement of failure planes are not observed. In Fig. 10, the relationship between tangential stresses and slip used in the CZM model is given. Further details about the use of CZM model in timber can be found in [6].

In ANSYS [1] the CZM model approach is applied by using the experimentally determined CZM model parameters. In ANSYS [1], the main input parameters to define the CZM model for the direction parallel to contact surface are given in Table 7. The elasto-plastic material behaviors on the bonded surfaces are simulated through the use of Cohesive Zone Modelling (CZM) in ANSYS which is mainly developed for the behavior of contact surfaces. The material model used in the modeling approach is given in

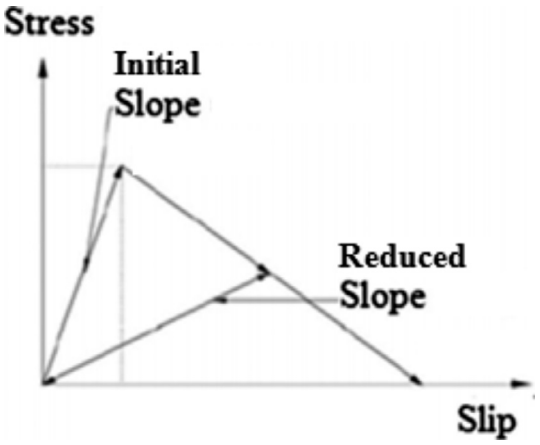

Fig. 10. Tangential stress and slip relationship used in the CZM model.

Fig. 10. The variation of model parameters in relation to the test variables (i.e., net and adhesive type) are given in Table 7. From the literature review, it is found that this approach is generally used for the simulation of experimentally tested bonding surfaces. The CZM model may be also used for the simulation of bonding surfaces between CFRP and concrete. In this study, this technique is used for the simulation of bonding surfaces of glulam beams. These parameters are extracted from the unpublished test results of the authors.

In the simulation of CZM model surface to surface modeling technique is applied by using the contact and target pairs from the ANSYS [1] library. The contact pairs capable of simulating the delamination behavior are used in this study to simulate the delamination of timber layers. CONTA174 may be used to represent contact and sliding between the surfaces subjected to delamination. CONTA174 has three translational degrees of freedom DOF) at each node. Contact occurs when the element surface penetrates one of the target elements on a specified target surface [1]. Similarly, TARGE170 may be used to represent target surfaces with the linked contact element [1]. Location of contact regions on a five layered test specimens is given in Fig. 11.

5. Comparison of numerical and experimental results

In this section the results obtained from the tests and finite element simulations are comparatively presented in terms of ultimate load capacities of test specimens. Typical stress distributions on

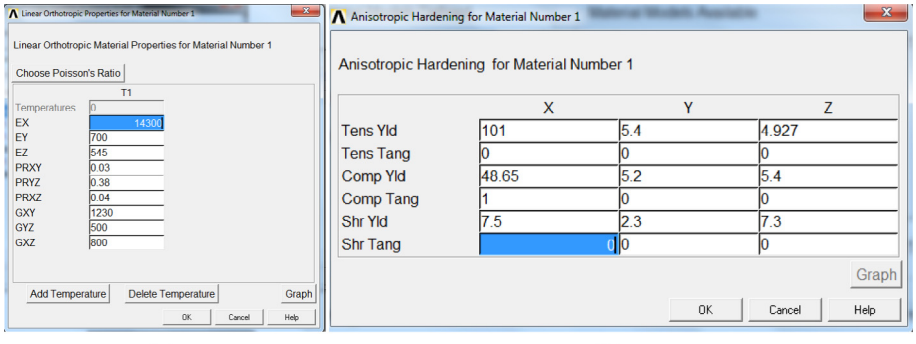

(a) (b)

Fig. 9. (a) Linear orthotropic and (b) anisotropic hardening model parameters used in the simulation of timber, in MPa.

Table 7
Parameters used in the CZM model.

Net Type	Glue Type	Maximum Shear Stress (MPa)	Maximum Slip Displacement (mm)	Stiffness (N/mm^3)
–	Epoxy	1.73	15.41	0.35
Aluminium	Epoxy	1.83	11.28	0.56
Fiber	Epoxy	2.03	8.40	0.67
Steel	Epoxy	2.14	8.08	0.69
–	Polyurethane	1.60	25.57	0.31
Aluminium	Polyurethane	1.75	22.55	0.54
Fiber	Polyurethane	1.98	16.64	0.64
Steel	Polyurethane	2.06	14.95	0.64

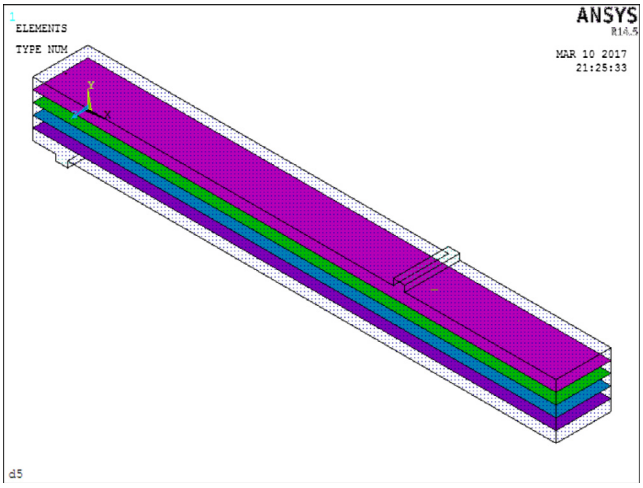

Fig. 11. Location of contact surfaces in a five layered test specimen.

the simulated test specimens are presented in Fig. 12a for a three layered beamand Fig. 12**b** for a five layered beam. Concentration of principal stresses close to the lower surface of the test specimens may be observed together with the local stress concentrations at the lamination surfaces (Fig. 12**c**).

The comparative results in terms of load carrying capacities are presented in Table 8. From the comparative presentation of the results it is observed that the finite element models fail to predict the relatively low load values (i.e., error% > 20). On the other hand, the error range in the predictions of test specimens with relatively low load values is acceptable (i.e., error% < 10). Such variations in the predictions indicate that the material model and failure criteria used in the finite element models should be improved. However, in the library of the used finite element software, there is no fully applicable material model and failure criteria that is specially developed for the simulation of timber structures. The load bearing values calculated by using finite element analyses were generally smaller than their experimental counterparts. The analyses results of test specimens without nets were more accurate than those of the others.

However, higher errors were observed from the analyses of specimens with nets. In all finite element analyses, the test specimens exhibit a more rigid behavior than their experimental counterparts. As in the case of load bearing capacities, the stiffness values of specimens without any nets very more accurately estimated than those of specimens with nets. In the finite element simulations, the failure is defined by assuming that the beam fails when the tension stresses at the outermost lamination reaches to the 80% of the tension capacity [10]. In relation to that all the failure modes are identified as tension face rupture.

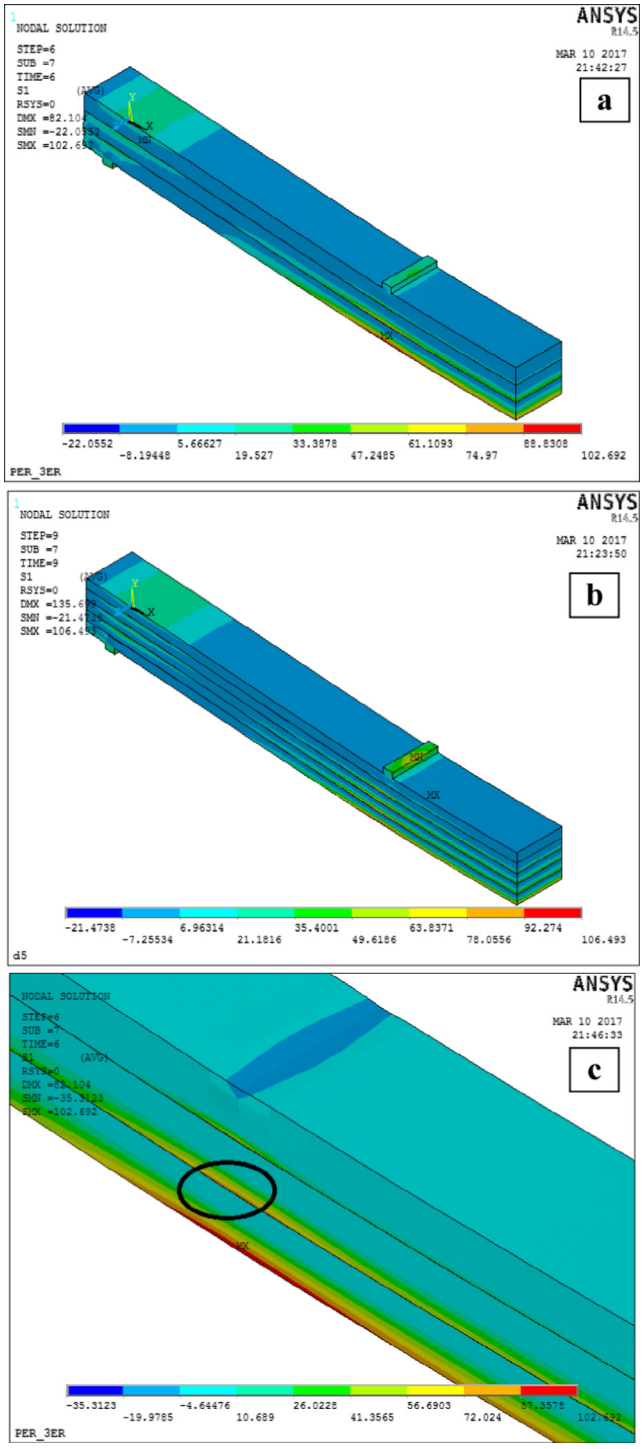

Fig. 12. Typical stress distribution at the instance of failure for (a) three layered glulam beam and (b) five layered glulam beam (c) concentration of stress at the outermost lamination surface (Stress Units is MPa).

6. Conclusions

In scope of this study, four point bending load tests were performer on glue laminated timber beams retrofitted using various types nets at the lamination surfaces. The experimental results are then evaluated in terms of load – displacement relationships, maximum load bearing capacity, initial stiffness, displacement ductility ratio, energy dissipation capacity and failure mechanism. In the study, effects of considered main variables (i.e., number of

Table 8
Comparison of experimental and numerical results.

Specimen No	Definition	Ultimate Capacity (kN)			Initial Stiffness (kN/mm)		
		Exper.	FEA	Error (%)	Exper.	FEA	Error (%)
1	PER_3ER	29.73	30	1	1.09	1.11	2
2	PER_3EA	34.57	33	5	1.30	1.37	6
3	PER_3EF	35.79	35	2	1.35	1.39	3
4	PER_3ES	38.22	35	9	1.43	1.58	10
5	PER_3PR	29.70	29	2	1.07	1.11	3
6	PER_3PA	37.27	34	10	1.27	1.40	11
7	PER_3PF	44.03	34	30	1.31	1.71	31
8	PER_3PS	45.85	36	27	1.36	1.75	28
9	PER_5ER	29.83	28	7	1.17	1.26	8
10	PER_5EA	39.17	31	26	1.32	1.68	27
11	PER_5EF	42.91	33	30	1.38	1.81	31
12	PER_5ES	45.12	34	33	1.44	1.93	34
13	PER_5PR	29.81	27	10	1.14	1.27	11
14	PER_5PA	40.63	30	35	1.31	1.79	36
15	PER_5PF	44.41	32	39	1.36	1.90	40
16	PER_5PS	46.02	32	44	1.39	2.01	45

laminated layers, thickness of laminated layers, net type, glue type and loading direction) on the variation of stated performance parameters are investigated. In the literature, although there are studies focused on the behavior of glue laminated beams retrofitted with CFRP or steel members, there are no studies performed by the application of nets on the lamination surfaces. In relation it is believed that the experimental results of this study will contribute to the subject area.

From the experimental results it is revealed that the use of nets on the lamination surfaces increased the performance of the test specimens in terms of considered performance parameters (i.e., load–displacement relationships, maximum load bearing capacity, initial stiffness, displacement ductility ratio, energy dissipation capacity and failure mechanism) relative to the performance of unretrofitted test specimens. Use of retrofitting nets resulted in 34%, 31%, 21% and 14% increases in terms of load bearing capacity, initial stiffness ratio, displacement ductility ratio and energy dissipation capacity of test specimens, respectively. It should be noted that the retrofitting of test specimens increased the initial stiffness and load bearing capacities together with the displacement ductility ratio and energy dissipation capacity. Manufacturing and using of such glue laminated and retrofitted timber beams are very practical and do not necessitate any specialized workmanship or detailed work. Just the use of retrofitting nets increased the load bearing capacities significantly (i.e., 34%). Use of such retrofitted glue laminated beams will allow passing of larger openings by timber elements. The highest performance in terms of considered structural parameters was obtained from the specimens retrofitted using steel wire nets. The authors plan to perform the reverse cyclic loading tests of such glue laminated beams to further investigate the behavior and also plan to make a patent application. Applied retrofitting technique significantly increased the load bearing capacity of glulam beams. It is a practical, fast and feasible technique which may be applied during the production stage of glulam beams. Using this technique enable the crossing of larger openings with elements of smaller dimensions. In this way, a significant amount of wood, used in production, saved and the damage to the environment and the cost is reduced by consuming less wood.

A failure mechanism on the bonding surfaces is not observed in all test specimens except specimens with 5 layers. Actually, this conclusion indicates that the applied retrofitting procedure increased the bond strength between the layers. The applied retrofitting method not only increased the bonding stress but also increased load bearing capacity of the composite material formed by the net and the timber. The net used for the retrofitting also resisted some load.

In scope of the study also the nonlinear finite element analyses of the test specimens were performed by using the software ANSYS [1]. Performed literature review illustrated the lack of comprehensive finite element simulations, with accurate failure models and mechanisms, of such glue laminated beams with contact issues. Also, the lack of well known failure models, specially developed for loading conditions parallel to the lamination surfaces and for members with retrofitting nets, prevented conducting the finite element analyses of test specimens loaded in parallel direction to the lamination surfaces. For the loading condition perpendicular to the lamination surfaces, the error of the finite element simulations are observed in the range of 2% and 26% with a mean value of 14%. In order to increase the accuracy of the finite element models developed for the simulation of glue laminated beams, studies focused on the appropriate failure mechanisms and CZM models for timber should be performed.

References

[1] ANSYS Release 14.5 Documentation for ANSYS—Theory Reference for ANSYS and ANSYS Workbench, 2012, Canonsburg, PA.
[2] B. Anshari, Z.W. Guan, Q.Y. Wangc, Modelling of Glulam beams pre-stressed by compressed wood, Compos. Struct. 165 (2017) 160–170.
[3] B. Anshari, Z.W. Guan, A. Kitamori, K. Jung, K. Komatsu, Structural behaviour of glued laminated timber beams pre-stressed by compressed wood, Constr Build Mater 29 (2012) 24–32.
[4] P. Dietsch, T. Tannert, Assessing the integrity of glued-laminated timber elements, Constr. Build. Mater. 101 (2015) 1259–1270.
[5] R.H. Falk, Wood as a sustainable building material, in: R.J. Ross (Ed.), Wood handbook—Wood as an engineering material.Centennial Edition, Department of Agriculture, Forest Service, Forest Products Laboratory, Madison, WI: U.S., 2010, p. 1.
[6] B. Franke, P. Quenneville, Numerical modeling of the failure behavior of dowel connections in wood, J. Eng. Mech. 137 (3) (2011) 186–195.
[7] M. Fossetti, G. Minafò, M. Papia, Flexural behaviour of glulam timber beams reinforced with FRP cords, Constr. Build. Mater. 95 (2015) 54–64.
[8] M. Frese, H.S. Blaß, Characteristic bending strength of beech glulam, Mater. Struct. 40 (2006) 3–13.
[9] M. Haiman, K. Pavković, B. Baljkas, Application of Glulam Beam Girders With External Pre-Stressing, WTCE, World Conference on Timber Engineering, 2010.
[10] T. Juricek, Analysis of composite beams bases on wood and reinforced fibers, Slovak J. Civ. Eng. 4 (2009) 13–21.
[11] A. Kermani, Structural Timber Design, Blackwell Science Ltd., Cambridge, 1999, pp. 82–83.
[12] L. Weidong, Z. Ling, Q. Geng, W. Liu, H. Yang, K. Yue, Study on flexural behaviour of glulam beams reinforced by Near Surface Mounted (NSM) CFRP laminates, Constr. Build. Mater. 91 (2015) 23–31.
[13] D.M. Moses, H.G.L. Prion, Anisotropic plasticity and failure prediction in wood composites, Paper presentation for ANSYS Inc. Ninth International Conference and Exhibition, August 2000, 2000.
[14] R.C. Moody, A. TenWolde, Use of Wood in Buildings and Bridges Wood Handbook – Wood as an Engineering Material, U.S. Department of Agriculture, Forest Service, Forest Products Laboratory Madison, 1999. pp. 16-1.
[15] S.W. Nunnally, Construction Methods and Management, seventh ed., Pearson Prentice Hall, New Jersy, 2007, p. 295.

[16] J. Pencik, Modelling of experimental tests of wooden specimens from scots pine (Pinus sylvestris) with the help of anisotropic plasticity material model, DrvnaIndustrija 66 (1) (2015) 27–33.
[17] G.M. Raftery, P.D. Rodd, FRP reinforcement of low-grade glulam timber bonded with wood adhesive, Constr. Build. Mater. 91 (2015) 116–125.
[18] G.M. Raftery, A.M. Harte, Nonlinear numerical modelling of FRP reinforced glued laminated timber, Compos. B 52 (2013) 40–50.
[19] J. Sena-Cruz, M. Jorge, J.M. Branco, V.M.C.F. Cunha, Bond between glulam and NSM CFRP laminates, Constr. Build. Mater. 40 (2013) 260–269.
[20] N.M. Stark, Z. Cai, C. Carll, Wood-based composite materials, panel products, glued-laminated timber, structural composite lumber, and wood–nonwood composite materials, in: R.J. Ross (Ed.), Wood handbook—Wood as an Engineering Material, Department of Agriculture, Forest Service, Forest Products Laboratory, Madison, WI, U.S., 2010. pp. 11-1,11-2,11-17,11-20.
[21] J.J. Stalnaker, E.C. Harris, Structural Design in Wood, second ed., Massachusetts: Kluwer Academic Publishers, 1999. 11-12, 17-18, 157-159,305.
[22] V.D. Tran, M. Oudjene, P.J. Méausoone, Experimental and numerical analyses of the structural response of adhesively reconstituted beech timber beams, Compos. Struct. 119 (2015) 206–217.
[23] S. Thelandersson, Timber Engineering - General Introduction, in: S. Thelandersson, H.J. Larsen (Eds.), Timber Engineering, John Wiley & Sons Ltd., West Sussex, 2003, p. 7.
[24] H. Yang, W. Liu, X. Ren, A component method for moment-resistant glulam beam–column connections with glued-in steel rods, Eng. Struct. 115 (2016) 42–54.
[25] H. Yang, D. Ju, W. Liu, W. Lu, Prestressed glulam beams reinforced with CFRP bars, Constr. Build. Mater. 109 (2016) 73–83.